LAWRENCE
LIVERMORE
NATIONAL
LABORATORY

LLNL-JRNL-478411

Numerical Error Estimation for Nonlinear Hyperbolic PDEs via Nonlinear Error Transport

J. W. Banks, J. A. F. Hittinger, J. M. Connors, C. S. Woodward

April 4, 2011

Computer Methods in Applied Mechanics and Engineering

Disclaimer

This document was prepared as an account of work sponsored by an agency of the United States government. Neither the United States government nor Lawrence Livermore National Security, LLC, nor any of their employees makes any warranty, expressed or implied, or assumes any legal liability or responsibility for the accuracy, completeness, or usefulness of any information, apparatus, product, or process disclosed, or represents that its use would not infringe privately owned rights. Reference herein to any specific commercial product, process, or service by trade name, trademark, manufacturer, or otherwise does not necessarily constitute or imply its endorsement, recommendation, or favoring by the United States government or Lawrence Livermore National Security, LLC. The views and opinions of authors expressed herein do not necessarily state or reflect those of the United States government or Lawrence Livermore National Security, LLC, and shall not be used for advertising or product endorsement purposes.

Numerical Error Estimation for Nonlinear Hyperbolic PDEs via Error Evolution[☆]

J. W. Banks[*], J. A. F. Hittinger, J. M. Connors, C. S. Woodward

Center for Applied Scientific Computing,
Lawrence Livermore National Laboratory,
Livermore, California, 94551

Abstract

The estimation of discretization error in numerical simulations is a key component in the development of uncertainty quantification. In particular, there exists a need for reliable, robust estimators for finite volume and finite difference discretizations of hyperbolic partial differential equations. The approach espoused here, often called the error transport approach in the literature, is to solve an auxiliary error equation concurrently with the primal governing equation to obtain a point-wise (cell-wise) estimate of the discretization error. One-dimensional, nonlinear, time-dependent problems are considered. In contrast to previous work, fully nonlinear error equations are advanced, and potential benefits are identified. A systematic approach to approximate the local residual for both method-of-lines and space-time discretizations is developed. Behavior of the error estimates on problems that include weak solutions demonstrates that this nonlinear error evolution provides useful error estimates.

Keywords: a posteriori error estimation, hyperbolic equations, finite volume methods, finite difference methods, weak solutions

[☆]This work was performed under the auspices of the U.S. Department of Energy by Lawrence Livermore National Laboratory under Contract DE-AC52-07NA27344 and was funded by the Uncertainty Quantification Strategic Initiative Laboratory Directed Research and Development Project at LLNL under project tracking code 10-SI-013.

[*]Corresponding author

Email addresses: banks20@llnl.gov (J. W. Banks), hittinger1@llnl.gov (J. A. F. Hittinger), connors4@llnl.gov (J. M. Connors), woodward6@llnl.gov (C. S. Woodward)

1. Introduction

For decades, numerical methods of increasing sophistication have been routinely and successfully used to compute approximate solutions to time-dependent differential equations. Concurrently, methods have been developed to estimate the approximation error of such discrete solutions. These *a posteriori* error estimation techniques have been traditionally used as *indicators* for mesh (element) adaptivity in an attempt to reduce discretization error by employing locally finer meshes. However, the increasing emphasis on Uncertainty Quantification (UQ) for numerical simulations presents a new challenge for robust, reliable, and accurate error *estimators* targeted at specific quantities of interest (QoI) derived from a simulation. Computational simulation typically introduces discretization error, and the uncertainty in computed results due to this error must be understood for proper interpretation of uncertainty analyses resulting from other input and data uncertainties.

In this paper, we are specifically interested in evolutionary methods of error estimation for finite difference method (FDM) and finite volume method (FVM) discretizations. In this error estimation approach, auxiliary evolution equations for the errors are derived, discretized, and solved in tandem with the approximate primal equations. Therefore, the computational cost is approximately twice that of solving the primal equation. The result is a discrete, signed, point-wise (cell-wise) approximation of the error that can be used subsequently to construct any number of linear or nonlinear functionals of the solution (QoIs). The effects of both error generation (destruction) and propagation are included, and, in addition, cancellation of errors in the calculation of QoIs can be obtained. In addition, when properly formulated, the nonlinear error transport approach is asymptotically correct and provides robust error estimates even for approximations of weak solutions.

Many approaches exist for global error estimation for numerical approximation of differential equations [1]. Historically, the main objective of error estimation has been to obtain a more accurate approximate solution by correcting a low-order scheme instead of resorting to a more expensive and potentially less robust higher-order discretization. Within the context of interest here, that is, providing error bounds on a discrete solution or functionals thereof, a basic comparison is provided in Roache [2]. Probably the most

common technique for FDM and FVM is the venerable mesh-refinement-based Richardson extrapolation [3]. In this approach solutions are computed on at least three meshes in order to fit the free parameters in an asymptotic error *ansatz*, typically an assumed power-law form. Grid convergence error estimation has the advantage that no modifications to the code are required, although care must be taken to constrain all code inputs properly to obtain self-consistent results. Richardson extrapolation may produce erroneous results if the error *ansatz* inadequately describes the true error behavior [2], which unfortunately may be the case for simulations that fail to resolve all scales in the solution. This includes cases where discontinuities are present and true weak solutions are sought. There have been attempts to consider richer *ansätze* with varying degrees of success [4].

In contrast to the mesh refinement strategy, several other classes of *single-grid* estimators exist. The finite element method (FEM) literature provides at least two broad classes of error estimators developed primarily for linear elliptic and parabolic problems: residual methods and recovery methods [5]. Typically these methods are used to produce error indicators for adaptive mesh refinement, and as such the error estimates are provided as local or global bounds in some relevant norm. Because of our focus on FDM and FVM discretizations of hyperbolic problems and of our interest in constructing error estimates in functionals of the solution, we do not consider these methods further.

Another class of single-grid estimators is based on the solution of auxiliary problems. Richardson extrapolation, for instance, can be based on varying the discretization order (*cf.*, mesh refinement) [2]. Such an approach has not often been used for finite difference and finite volume methods, most likely because of the difficulty of implementing multiple, higher-order and stable discretizations. Adjoint methods [6, 7] estimate the error in a QoI from the solution of an auxiliary adjoint problem and the residual of the discrete solution. When coupled with mesh adaptivity, for a small number of QoIs, adjoint methods can be very efficient, but the challenge of formulating the adjoint problem and the inefficiency of the approach if large numbers of QoI are desired can be drawbacks. With implicit residual methods [5, 8] from the FEM literature, local error estimators are developed by solving auxiliary equations for the error on a mesh element or on a patch of elements. The local errors can also be used to construct a computable estimate of some global norm of the error. However, the development of the local error equations is

specific to finite element methods.

In the finite difference and finite volume literature, evolutionary error methods considered herein are often referred to as *error transport* methods. These techniques are a form of non-iterative difference or differential defect correction [1, 9]. In all cases in the error transport literature, the error equations are linearized, and the focus is typically on the approximation used to evaluate the local residual, that is, the local source (sink) of error that drives an error transport equation. Linear error transport techniques have been applied to linear and nonlinear models of advection [10, 11] and advection-diffusion [11–16] equations, subsonic and supersonic inviscid flow [10, 17, 18], and subsonic viscous flow [12, 16]. Most investigations have considered steady-state solutions [13–18], and only a few examples of time-dependent applications [10, 11] exist. A good review of previous work can be found in Hay and Visonneau [16].

In the context of this previous work, this paper has several goals. Our overarching goal is to investigate the viability of the nonlinear error transport approach as a strategy of *a posteriori* error estimation for the purposes of uncertainty quantification. We focus on time-dependent, nonlinear, hyperbolic problems that admit weak solutions and present a new, simplified procedure for approximate residual evaluation that is applicable to both method-of-lines and space-time discretizations. In addition, we argue that solving the full error equations, including any error nonlinearity, has potential advantages over the more traditional approach of linearization. We demonstrate instances where the inclusion of these terms increases the robustness of the error estimates. Finally, we compare evolutionary estimates with those obtained by Richardson extrapolation to demonstrate the relative utility of the approach.

The remainder of this paper is structured as follows. In Section 2, we will introduce the basic concepts of nonlinear error transport for general time-dependent partial differential equations (PDEs), and in Section 3, we will present the core ideas of our approach in contrast to previous linear error transport work. We will specialize in Section 4 to a canonical example of a non-linear hyperbolic PDE, the 1D inviscid Burgers' equation. Specific example discretizations for both method-of-lines and space-time discretizations are developed. Properties of the method are experimentally demonstrated in Section 5 for strong and weak solutions, and the effects of nonlinearity in the error equation are explored. In Section 6, we demonstrate the application

of the approach to the 1D Euler system of nonlinear equations. Finally, we summarize our results and make conclusions in Section 7.

2. Basic Concepts

Consider an evolution equation for solution $u(x,t)$ of the form

$$\partial_t u + \mathcal{F}(u) = s, \tag{1}$$

where $\mathcal{F}(u)$ is some linear or nonlinear (spatial) differential operator on u and $s(x,t)$ is an inhomogeneous term. For convenience, we make the simplifying assumption that $x \in \mathbb{R}$ in order to eliminate the need to consider boundary conditions. The nature of errors introduced via boundary condition approximation is a rather interesting subject that will be addressed in future work. Initial conditions are given as $u(x, t=0) = g(x)$.

We now assume that we have a function $\tilde{u}(x,t)$ that approximates u but does not satisfy (1) exactly. Define the approximation error to be

$$e(x,t) = u(x,t) - \tilde{u}(x,t). \tag{2}$$

Substitution into (1) yields

$$\partial_t e + \mathcal{F}(e + \tilde{u}) = s - \partial_t \tilde{u}. \tag{3}$$

A residual is formed on the right-hand side by subtracting $\mathcal{F}(\tilde{u})$ from both sides:

$$\partial_t e + \mathcal{G}(e; \tilde{u}) = -\left(\partial_t \tilde{u} + \mathcal{F}(\tilde{u}) - s\right), \tag{4}$$

where $\mathcal{G}(e; \tilde{u}) = \mathcal{F}(e + \tilde{u}) - \mathcal{F}(\tilde{u})$. The reason for this last step becomes apparent when $\mathcal{F}$ is restricted to be a linear operator; in this case,

$$\partial_t e + \mathcal{F}(e) = -\left(\partial_t \tilde{u} + \mathcal{F}(\tilde{u}) - s\right), \tag{5}$$

that is, the error is acted on by the same operator as the primal solution and driven by the residual of that operator acting on the approximate solution. Though obfuscated somewhat by the explicit time derivative and nonlinear generalization, the relationship in (4) (or more often (5)) between error and residual are a well-known result in numerical analysis.

Equation (4) is the error equation that describes the evolution of the approximation error in space and time. The source of error is the residual

of the approximate solution, and, in the nonlinear case, the error evolves by a *different* differential operator than the solution. In the linear error transport approach [10–18], the differential operator on the left-hand side of (4) is linearized about $\tilde{u}$, which is a reasonable assumption so long as $|e(x,t)| \ll |u(x,t)|$. In practice, and in some very important cases, this is not valid, and such a linearization becomes questionable. We will demonstrate some of these failings in Section 5 and show that use of the nonlinear error transport equation overcomes these problems.

Through this point in the discussion, $\tilde{u}$ and e have been treated as continuous functions of x and t. We now specialize to the problem of discretization error. In general, we do not know how to solve either the original PDE (1) or the error equation (4). We can, however, discretize both and solve each approximately. There are thus three decisions to be made: the choice of discretization of the primal equation (1), the choice of discretization of the evolution operator in the error equation (4), and the choice of an evaluation technique for the residual in the error equation (4). Appropriate choices for the first two discretizations depend intimately on the nature of the continuous operator and initial conditions. Typically the same (or a similar) scheme is used for both the primal and auxiliary equations.

In the best case of, smooth solutions and consistent, stable, solution-independent discretizations, we can determine the relationship of the order of the three discretizations to the rate of convergence of the error approximation. Of course, for weak solutions or nonlinear schemes, this relationship will provide only an upper bound. We take a finite-difference viewpoint with $u_i^n = u(x_i, t^n)$ and assume a smooth (infinitely differentiable) exact solution and numerical approximation; similar constructions can be made in the finite-volume framework. We also assume $\Delta x / \Delta t$ is fixed as $\Delta x, \Delta t \to 0$ in order to simplify notation. We assume that the primal scheme is order p_t in time and p_x in space, *i.e.*,

$$|e| = |\tilde{u} - u| = O(\Delta t^{p_t}) + O(\Delta x^{p_x}) = O(\Delta x^p)\,, \tag{6}$$

where $p = \min(p_t, p_x) > 0$. We write the discretization of the error equation as

$$\frac{\tilde{e}_i^{n+1} - \tilde{e}_i^n}{\Delta t} + G_i\left(\tilde{e}^n; \tilde{u}^n, \tilde{u}^{n+1}\right) = -R\left(\tilde{u}^n, \tilde{u}^{n+1}\right).$$

If the left-hand side of the discrete error equation is order q_t in time and q_x

in space, and we set $q = \min(q_t, q_x) > 0$, then Taylor series expansion gives

$$[\partial_t \tilde{e} + \mathcal{G}(\tilde{e}; \tilde{u})]_i^n = O(\tilde{e}\Delta x^q) = O\big(\Delta x^{p+q}\big).$$

The $\tilde{e}$ factor appears because the Taylor series terms are derivatives of $\tilde{e}$, we have assumed that the solution is well-resolved, and $\tilde{e}$ approximates e, which by (6) is an $O(\Delta x^p)$ quantity. Assume the residual is approximated to order r_t in time and r_x in space with $r = \min(r_t, r_x) > 0$:

$$R\left(\tilde{u}^n, \tilde{u}^{n+1}\right) = \mathcal{R}(\tilde{u})|_i^n + O(\Delta x^r).$$

Thus,

$$[\partial_t \tilde{e} + \mathcal{G}(\tilde{e}; \tilde{u}) - \mathcal{R}(\tilde{u})]_i^n = O\big(\Delta x^{p+q}\big) + O(\Delta x^r),$$

and so the rate of convergence of the approximate error $\tilde{e}$ is

$$|\tilde{e} - e| = O\big(\Delta x^{\min(p+q,r)}\big). \tag{7}$$

The ratio

$$\frac{||\tilde{e}||}{||\tilde{u} - u||} = 1 + O\big(\Delta x^{\min(q,r-p)}\big)$$

indicates that under the assumed conditions, the error estimate will be asymptotically correct so long as $r > p$. Therefore, the use of the same orders for primal and error equation discretizations results in asymptotically correct error estimates so long as the residual approximation is sufficiently accurate, as demonstrated in [10, 16].

The evaluation of the residual has been a primary focus of investigation in the literature to date. This issue arises for FDM and FVM schemes because of the discrete nature of the approximate solution to the primal equation. Thus, the residual operator must be approximated by some discrete difference operator acting on the approximate primal solution, or the approximate primal solution must be reconstructed into a continuous function to be acted upon by the continuous differential residual operator. Either way, additional approximation error is introduced that must be smaller than the local truncation error of the primal discretization.

As identified by Hay and Visonneau [16], which provides a very good review of the application of error transport methods to computational fluid dynamics, there are three approaches commonly taken:

1. Approximate the residual by a discretization;

2. Approximate the residual by one or more leading truncation error terms from the modified differential equation of the primal discretization [10, 17];
3. Approximate the residual by reconstructing the approximate solution and directly applying the differential residual operator [12, 16, 19, 20].

The first is the standard approach for more traditional uses of defect correction [9, 19, 20] and requires the use of a different and typically high-order discretization than used in the primal equation. However, because the residual represents a local source of error as a function of the approximate primal solution and not the error itself, stability of the error discretization is largely independent of the specifics of the discrete residual operator. This is the approach we adopt because of its relative simplicity for logically rectangular Cartesian or curvilinear grids. The second choice relies on the asymptotic equivalence of the residual (differential operator applied to the discrete solution) and truncation error (difference operator applied to the continuous solution). Typically, only the leading-order truncation error term is used. This approach can be challenging because the truncation error for many modern nonlinear discretizations can be difficult to derive and/or evaluate numerically. As a further complication, there are cases where the error behavior is not well represented by the first-order term and so two or more terms of the truncation error may have to be used. The final approach requires interpolants of order sufficient to provide both the necessary derivatives and accuracy as well as consistency with any initial or boundary conditions. We note that asymptotically, all of these approaches are equivalent, and that, in the case of linear operators, every choice of linear reconstruction (Option 3) leads to a particular choice of linear discretization (Option 1).

Before proceeding to the specifics of our residual evaluation strategy for method-of-lines and space-time discretizations, we will remark that another error transport approach exists in the literature. Our formalism is based on the continuous error equation that has been referred to in the literature as "Continuous Error Transport Equation" or "Exact Operator Residual" methods. In contrast and in a completely analogous way, one can develop a discrete error equation directly by beginning with the difference equation solved exactly by the discrete solution and introducing a discrete form of (2). In this case, the error equation is driven by the truncation error instead of the residual, but the evaluation of the source term is still an important issue [11, 13–15, 18]. Such methods have been referred to as "Discrete Error Transport

Equation" or "Approximate Operator Residual" methods. Asymptotically, the two approaches are equivalent.

3. Residual Evaluation

Because of the dependence in time, we adopt the approach of using a discrete approximation of the residual. We wish to avoid explicit interpolation in time that would be necessary in a direct reconstruction method [12, 16, 19, 20]. Furthermore, approximation of the residual by leading-order truncation error terms [10, 17] is not only scheme-specific and difficult for complex problems, but also potentially less robust for under-resolved features where neglected terms may not be negligible. We consider two types of discretization approaches common for hyperbolic PDEs: the method-of-lines approach, where space is discretized first and then an appropriate ODE discretization is applied in time, and the space-time approach, where schemes take advantage of the coupled nature of time and space in hyperbolic problems to cancel leading spatial error terms with leading temporal error terms. In this section, we give a general overview of the two approaches. Specific examples of each for a model problem are provided in Section 4.

3.1. Method-of-Lines Formulation

The method-of-lines formulation provides a conceptually simple approach to the high-order discretization of time-dependent problems because of the independent treatment of space and time. Indeed, one of the original and popular approaches to the discretization of the Euler equations combined a central second-order spatial discretization with the explicit, four-stage fourth-order Runge-Kutta scheme [21]. We show that the method-of-lines formulation allows for a particularly simple evaluation of the residual.

We discretize the spatial operator of the primal equation (1) to obtain the semi-discrete form

$$\partial_t \tilde{u}_h + F_h(\tilde{u}_h) = 0, \tag{8}$$

where F_h is some discrete operator that acts on one or more time levels, h is the spatial discretization parameter, and $\tilde{u}_h(t)$ is a vector of time-dependent variables.

Of course, if we cannot solve the primal equation (1), it is unlikely that we can solve the error equation (4). Thus, we will spatially discretize the

error equation:

$$\partial_t \tilde{e}_h + G_h(\tilde{e}_h; \tilde{u}_h) = -\partial_t \tilde{u}_h - F_h^*(\tilde{u}_h), \tag{9}$$

where G_h and F_h^* are discrete approximations of $\mathcal{G}$ and $\mathcal{F}$, respectively. Note that we do not assume that $G_h = F_h$. It should be made clear that the right-hand side discretization must not be the same discretization used for the primal equation, because the semi-discrete primal solution $\tilde{u}_h$ exactly solves that semi-discrete equation (8). To make this explicitly clear, using (8) in the right-hand side of (9), we find

$$\partial_t \tilde{e}_h + G_h(\tilde{e}_h; \tilde{u}_h) = F_h(\tilde{u}_h) - F_h^*(\tilde{u}_h). \tag{10}$$

Notice that the source of error vanishes for $F_h = F_h^*$. In addition, using (8) in (9) analytically eliminates the time derivative from the residual. To obtain a fully discrete scheme, one applies a suitable ODE integration and co-evolves the primal and error approximations.

3.2. Space-Time Formulation

For hyperbolic systems, it is common to discretize the primal equation using a space-time scheme, by which we mean a one-step scheme (possible with predictor stages) that couples the time and space discretizations. The Lax-Wendroff [22] and MUSCL-Hancock [23, 24] schemes are both of this type. The construction of space-time schemes is specific to the differential form of the spatial operator, but the general principle is that successive derivatives of the governing equation are used to exchange temporal with spatial derivatives in a Taylor series expansion in time. The resulting spatial derivatives are then discretized. A similar procedure can be used in the construction of a difference approximation to the residual in order to avoid a higher-order temporal discretization across multiple discrete time levels.

Because the extension to systems is not as clear for space-time formulations as it was for the method-of-lines in Section 3.1, we consider the more general hyperbolic system

$$\partial_t u + \partial_x f(u) = 0, \tag{11}$$

where $f(u)$ is a flux function whose Jacobian $\partial_u f$ has real eigenvalues. Note that the approach is by no means restricted to this form of operator and reduction to Burgers' equation is entirely straightforward.

Consider the residual for a continuous approximation to the solution of (11):

$$\mathcal{R}(\tilde{u}) = \partial_t \tilde{u} + \partial_x f(\tilde{u}). \tag{12}$$

Using the approximate solution at two time levels, $\tilde{u}(x,t^n)$ and $\tilde{u}(x,t^{n+1})$, we can construct the following second-order approximation of $\mathcal{R}(\tilde{u})$ at time $t = t^{n+1/2}$:

$$\frac{\tilde{u}(x,t^{n+1}) - \tilde{u}(x,t^n)}{\Delta t} + \partial_x \left(\frac{f\left(\tilde{u}(x,t^{n+1})\right) + f\left(\tilde{u}(x,t^n)\right)}{2} \right) = \left[\partial_t \tilde{u} + \partial_x f(\tilde{u}) - \frac{\Delta t^2}{12} \partial_{ttt} \tilde{u} \right]_{t^{n+1/2}} + O\left(\Delta t^4\right).$$

Rearranging, we have

$$\begin{aligned} \left[\partial_t \tilde{u} + \partial_x f(\tilde{u})\right]_{t^{n+1/2}} =& \frac{\tilde{u}(x,t^{n+1}) - \tilde{u}(x,t^n)}{\Delta t} \\ &+ \partial_x \left(\frac{f\left(\tilde{u}(x,t^{n+1})\right) + f\left(\tilde{u}(x,t^n)\right)}{2} \right) \\ &+ \frac{\Delta t^2}{12} \partial_{ttt} \tilde{u} \Big|_{t^{n+1/2}} + O\left(\Delta t^4\right). \end{aligned} \tag{13}$$

As an example, we use the primal equation to convert $\partial_{ttt} u$ into spatial derivatives; specifically,

$$\partial_t u = -\partial_x f(u), \tag{14a}$$

$$\partial_{tt} u = -\partial_{tx} f(u) = -\partial_x \left[A(u) \partial_t u\right] = \partial_x \left[A(u) \partial_x f(u)\right], \tag{14b}$$

$$\begin{aligned} \partial_{ttt} u &= \partial_{tx} \left[A(u) \partial_x f(u)\right], \\ &= \partial_x \left[\frac{\partial A}{\partial u} \partial_t u \partial_x f(u) + A(u) \partial_{tx} f(u) \right], \\ &= -\partial_x \left[\frac{\partial A}{\partial u} \left(\partial_x f(u)\right)^2 + A(u) \partial_x \left[A(u) \partial_x f(u)\right] \right]. \end{aligned} \tag{14c}$$

We thus can construct a formally fourth-order in time difference approxima-

tion of the residual at $t = t^{n+1/2}$ by combining (13) and (14c):

$$\begin{aligned}\mathcal{R}(\tilde{u}) \approx & \frac{\tilde{u}(x,t^{n+1}) - \tilde{u}(x,t^n)}{\Delta t} \\ & + \partial_x \left(\frac{f\left(\tilde{u}(x,t^{n+1})\right) + f\left(\tilde{u}(x,t^n)\right)}{2} \right) \\ & - \frac{\Delta t^2}{12} \partial_x \left[\frac{\partial A}{\partial u} \left(\partial_x f(\tilde{u})\right)^2 + A(\tilde{u}) \partial_x \left[A(\tilde{u}) \partial_x f(\tilde{u}) \right] \right]_{t^{n+1/2}} .\end{aligned} \tag{15}$$

Applying this approach to higher temporal derivatives in the Taylor series expansion leads to higher-order residual approximations in time. Appropriate spatial differences are subsequently used to approximate the spatial derivatives.

Again, we note that this process, though more complicated than that for the method-of-lines, generalizes. The core idea is to use Taylor series expansions in time and the primal equation to convert temporal derivatives in the expansion into spatial derivatives. These spatial derivatives are then approximated with appropriate spatial differencing, and the result is an increase in the temporal accuracy of the method. One insight used here is that it is easier to start with a lower-order temporal approximation and then use Taylor series analysis to identify the terms needed to further increase the formal accuracy.

Finally, we note that one-step space-time schemes are in practice seldom implemented as a single evaluation. Instead, much like a Runge-Kutta scheme, a multi-step, predictor-corrector approach is often employed. In such a predictor-corrector procedure, additional high-order approximations of the differential residual may be required, and these can be constructed using these same principles of Taylor series expansion and primal equation differentiation.

4. Model Nonlinear Problem: Inviscid Burgers' Equation

The linear error transport approach has been applied to the steady-state [12, 16–18] and time-dependent [10] Euler and Navier-Stokes systems that describe fluid flow. We are particularly interested in the time-dependent, nonlinear hyperbolic case because of its admission of weak solutions, but we wish to first restrict our consideration to a scalar equation for clarity. The

inviscid Burgers' equation,

$$\partial_t u + \partial_x \left(\frac{1}{2} u^2 \right) = 0, \qquad x \in \mathbb{R}, \quad t > 0, \tag{16}$$

is a logical model to consider because it possesses an advective nonlinearity similar to that of the Euler and Navier-Stokes models. We assume an initial value problem (IVP) with initial conditions given as $u(x, t = 0) = g(x)$. Solutions can be constructed using the method of characteristics; see, for instance Whitham [25].

In practice, strong solutions to (16) exist only for finite time. In particular, discontinuities can form when the solution steepens through nonlinear interaction. It is therefore common to consider solutions in a weak sense. For this reason, the divergence, or conservation, form (16) is commonly used. The continuous nonlinear error transport equation for an approximate solution $\tilde{u}(x, t)$ to the Burgers' equations is

$$\partial_t e + \partial_x \left(\frac{1}{2} e^2 \right) + \partial_x \left(\tilde{u} e \right) = -\partial_t \tilde{u} - \partial_x \left(\frac{1}{2} \tilde{u}^2 \right). \tag{17}$$

The left-hand side is a nonlinear and variable-coefficient advection operator applied to e. Both of the spatial derivative terms on the left-hand side can be large, with either one of them dominating in a particular region of the solution. As a result, both terms must be present in order to describe the time evolution of the error for some cases. The inclusion of the nonlinear term $\partial_x(e^2/2)$ distinguishes our nonlinear error transport approach from the linear error transport approach that has been used previously. In Section 5, we will demonstrate advantages of preserving the nonlinearity.

We consider conservative, upwind, finite-difference schemes [23] that are well suited to this class of problems. Both method-of-lines and space-time discretizations will be developed. Similar space-time schemes were employed in [10].

4.1. Method-Of-Lines Discretization

We explicitly specify our semi-discrete scheme for both the primal and error equations. Temporal discretization for all MOL discretizations throughout this paper is accomplished using the standard explicit, four-stage, fourth-order Runge-Kutta scheme.

4.1.1. Discretization of the Primal Equation

Consider a semi-discrete approximation of (16) on the uniform spatial grid $x_i = x_0 + i\Delta x$. Spatial approximation is indicated using a subscript (*e.g.*, $\tilde{u}_i(t) \approx \tilde{u}(x_i, t)$). A conservative spatial approximation for Burgers' equation can be written as

$$\partial_t \tilde{u}_i = -\frac{1}{2\Delta x} D_+ \left[(\tilde{u}_{i-1/2})^2 \right], \tag{18}$$

where $D_+[v_i] = v_{i+1} - v_i$ is the forward difference operator and where the $\tilde{u}_{i\pm 1/2}$ are determined through the solution of Riemann problems [25, 26] at cell faces. Specifically, if we define $\tilde{u}_{i-1,+}$ and $\tilde{u}_{i,-}$ to be the values at the left- and right- of the $(i-1/2)$ interface, respectively,

$$\tilde{u}_{i-1/2} = \begin{cases} \tilde{u}_{i-1,+}, & \text{if} \quad \tilde{u}_{i,-} > \tilde{u}_{i-1,+} > 0, \\ \tilde{u}_{i,-}, & \text{if} \quad 0 > \tilde{u}_{i,-} > \tilde{u}_{i-1,+}, \\ \tilde{u}_{i-1,+}, & \text{if} \quad \frac{1}{2}(\tilde{u}_{i-1,+} + \tilde{u}_{i,-}) > 0 \ \text{ and } \ \tilde{u}_{i,-} \leq \tilde{u}_{i-1,+}, \\ \tilde{u}_{i,-}, & \text{if} \quad \frac{1}{2}(\tilde{u}_{i-1,+} + \tilde{u}_{i,-}) \leq 0 \ \text{ and } \ \tilde{u}_{i,-} \leq \tilde{u}_{i-1,+}, \\ 0, & \text{otherwise.} \end{cases} \tag{19}$$

To increase the spatial order of accuracy, piecewise linear reconstruction over each cell is used to obtain improved approximations to the solution values $\tilde{u}_{i,\pm}$ at cell boundaries:

$$\tilde{u}_{i,\pm} = \tilde{u}_i \pm \frac{1}{2} \psi \left(D_+ \left[\tilde{u}_i \right], D_+ \left[\tilde{u}_{i-1} \right] \right).$$

The limiter function, $\psi(\cdot, \cdot)$, is used to change the character of the scheme. We will consider three choices for ψ:

$$\psi_1(u, v) = 0, \tag{20a}$$

$$\psi_2(u, v) = \frac{1}{2}(u + v), \tag{20b}$$

$$\psi_{MM}(u, v) = \text{minmod}\,(u, v), \tag{20c}$$

where

$$\text{minmod}\,(u, v) = \begin{cases} u, & \text{if } |u| < |v| \text{ and } uv > 0, \\ v, & \text{if } |u| \geq |v| \text{ and } uv > 0, \\ 0, & \text{if } uv \leq 0. \end{cases}$$

The first case will give a first-order upwind scheme, the second will give an unlimited second-order upwind scheme, and the third choice yields a total-variation-diminising (TVD), limited, high-resolution scheme [23, 27].

4.1.2. Discretization of the Error Equation

Consider now the numerical approximation of the error equation (17). As noted previously, in the finite-difference (finite-volume) framework, we are free to choose the discretization of the left-hand and the right-hand sides as desired under the constraint that the same discrete operator cannot be used for the right-hand side of the error equation as was used for the primal equation ($F_h \neq F_h^*$). There are other accuracy considerations; the residual should be evaluated at higher-order than the primal equation, and the error equation should be discretized at the same, or higher, order than the primal equation. Nevertheless, because the error does not appear in the right hand side of the error equation, we are free to choose high-order stencils without raising stability concerns.

The discretization of the differential residual

$$\mathcal{R}(\tilde{u}) = \partial_t \tilde{u} + \partial_x \left(\frac{1}{2} \tilde{u}^2 \right) \tag{21}$$

for Burgers' error equation (17) is relatively straight-forward. We assume that $\tilde{u}_i$ is a discrete approximation of $\tilde{u}$ that satisfies (18). Thus, following the discussion in Section 3.1, the primal discretization (18) provides a discrete expression of the first term in (21).

We can choose a discrete approximation of the second term in (21) that uses the same 5-point stencil required for (18). There are two obvious candidate fourth-order approximations: $\Delta x \partial_x \left(\tilde{u}^2 \right) \approx D_0^{(4)} \left[\tilde{u}_i^2 \right]$ and $\Delta x \partial_x \left(\tilde{u}^2 \right) \approx 2\tilde{u}_i D_0^{(4)} \left[\tilde{u}_i \right]$. Here $D_0^{(4)} = D_0 \left(1 - \frac{1}{6} D_+ D_- \right)$ is the fourth-order, undivided, first-difference operator. These two choices correspond to a conservative and a quasi-linear approximation of this term and will result in error approximations with different properties. From an accuracy perspective, a truncation error analysis reveals that

$$\frac{1}{2\Delta x} D_0^{(4)} \left[\tilde{u}_i^2 \right] = \partial_x \left(\tilde{u}^2 \right) - \frac{\Delta x^4}{30} \left(\tilde{u} \partial_x^5 \tilde{u} + 5 \partial_x \tilde{u} \partial_x^4 \tilde{u} + 10 \partial_x^2 \tilde{u} \partial_x^3 \tilde{u} \right) + \cdots$$

while

$$\frac{1}{\Delta x} \tilde{u}_i D_0^{(4)} \left[\tilde{u}_i \right] = \partial_x \left(\tilde{u}^2 \right) - \frac{\Delta x^4}{30} \left(\tilde{u} \partial_x^5 \tilde{u} \right) + \cdots .$$

For smooth solutions then the latter would typically be a better choice because of its generally smaller truncation error. For this case the discretization

of the right hand side is thus

$$\mathcal{R}(\tilde{u}_i) = -\frac{1}{2\Delta x} D_+ \left[(u_{i-1/2})^2 \right] + \frac{1}{\Delta x} u_i D_0^{(4)} \left[u_i \right] + O\left(\Delta x^4\right). \tag{22}$$

For weak solutions the conservative choice may be more appropriate which would lead to

$$\mathcal{R}(\tilde{u}_i) = -\frac{1}{2\Delta x} D_+ \left[(u_{i-1/2})^2 \right] + \frac{1}{2\Delta x} D_0^{(4)} \left[(u_i)^2 \right] + O\left(\Delta x^4\right). \tag{23}$$

Of course, other valid choices could be made.

The left hand side of (17) consists of the non-linear Burgers' term $\partial_x(e^2/2)$ and the non-constant-coefficient advection term $\partial_x(\tilde{u}e)$, representing non-linear and non-constant coefficient transport of e. We note that in this nonlinear case, this is not the same operator as in the primal Burgers' equation, but it is still amenable to a similar discretization strategy.

As was done for the primal equation, we consider the full left hand side of the error equation (17) in conservative form. Using the residual discretization (22), we form the semi-discrete, conservative, upwind scheme

$$\partial_t \tilde{e}_i = -\frac{1}{\Delta x} D_+ \left[\tilde{e}_{i-1/2} (\tilde{u}_{i-1/2} + \frac{1}{2} \tilde{e}_{i-1/2}) \right] + \mathcal{R}(\tilde{u}_i).$$

The definition of $\tilde{u}_{i\pm1/2}$ follows from the polynomial interpolant of $\tilde{u}$ from $\tilde{u}_i$ that is consistent with the discretization chosen in (22)

$$\tilde{u}_{i-1/2} = \frac{1}{16} \left(-\tilde{u}_{i-2} + 9\tilde{u}_{i-1} + 9\tilde{u}_i - \tilde{u}_{i+1} \right) + O\left(\Delta x^4\right).$$

The definition of $\tilde{e}_{i\pm1/2}$ is similar to the definition of $\tilde{u}_{i\pm1/2}$ in Section 4.1.1. Approximations to the error at the right and left cell boundaries are defined as

$$\tilde{e}_{i,\pm} = \tilde{e}_i \pm \frac{1}{2} \psi \left(D_+ \left[\tilde{e}_i \right], D_+ \left[\tilde{e}_{i-1} \right] \right).$$

Definitions of $\tilde{e}_{i\pm1/2}$ follow from the solution to the Riemann problem

$$\tilde{e}_{i-1/2} = \begin{cases} \tilde{e}_{i-1,+}, & \text{if} \quad \tilde{e}_{i,-} > \tilde{e}_{i-1,+} > \tilde{u}_{i-1/2}, \\ \tilde{e}_{i,-}, & \text{if} \quad \tilde{u}_{i-1/2} > \tilde{e}_{i,-} > \tilde{e}_{i-1,+}, \\ \tilde{e}_{i-1,+}, & \text{if} \quad \frac{1}{2}(\tilde{e}_{i-1,+} + \tilde{e}_{i,-}) > \tilde{u}_{i-1/2} \ \text{ and } \ \tilde{e}_{i,-} \leq \tilde{e}_{i-1,+}, \\ \tilde{e}_{i,-}, & \text{if} \quad \frac{1}{2}\tilde{e}_{i-1,+} + \tilde{e}_{i,-}) \leq \tilde{u}_{i-1/2} \ \text{ and } \ \tilde{e}_{i,-} \leq \tilde{e}_{i-1,+}, \\ 0, & \text{otherwise.} \end{cases}$$

4.2. Space-Time Formulation

We will use a MUSCL-Hancock approach that makes use of a spatial discretization having many features in common with our method-of-lines formulation.

4.2.1. Discretization of the Primal Equation

For Burgers' equation, we write the fully discrete, conservative updates in the form

$$\tilde{u}_i^{n+1} = \tilde{u}_i^n - \frac{\Delta t}{2\Delta x} D_+ \left[\left(\tilde{u}_{i-1/2}^{n+1/2} \right)^2 \right]. \tag{24}$$

Here $\tilde{u}_{i-1/2}^{n+1/2}$ is found as the solution to the Riemann problem (19) with left and right inputs evaluated at the mid-time level. These left and right states are defined through Taylor expansion in both space and time; formally, to second-order in space and time,

$$\tilde{u}_{i,\pm}^{n+1/2} = \tilde{u}_i^n + \frac{1}{2} \left(\pm 1 - \frac{\tilde{u}_i^n \Delta t}{\Delta x} \right) \psi \left(D_+ \left[\tilde{u}_i^n \right], D_+ \left[\tilde{u}_{i-1}^n \right] \right).$$

4.2.2. Discretization of the Error Equation

In order for the eventual discretization of the error equation to be higher-order accurate for smooth flows (as was the case for the method of lines discretization), the discretization of the transport terms must be at least as accurate as the primal discretization. Here we are considering second-order primal discretizations, and so a second order Hancock scheme for the error equation can be written as

$$\tilde{e}_i^{n+1} = \tilde{e}_i^n - \frac{\Delta t}{2\Delta x} D_+ \left[\left(\tilde{e}_{i-1/2}^{n+1/2} \right)^2 \right] - \Delta t R_i^{n+1/2}.$$

We must still specify $\tilde{e}_{i-1/2}^{n+1/2}$ and $R_i^{n+1/2}$ with sufficient accuracy.

Consider $R(\tilde{u}_i^{n+1/2})$ first. Following the approach from Section 3.2, we first construct an approximation using only two time levels. In order to provide for up to fourth order accuracy for the error, a third order accurate approximation for $\mathcal{R}(\tilde{u})$ must be devised. The primal governing equation can be used to determine the following:

$$\partial_t^3 u = -6u(\partial_x u)^3 - 9u^2 \partial_x u \partial_x^2 u - u^3 \partial_x^3 u. \tag{25}$$

Thus, the residual can be approximated to third order accuracy as

$$\begin{aligned} R_i^{n+1/2} =& \frac{\tilde{u}_i^{n+1} - \tilde{u}_i^n}{\Delta t} \\ &+ \frac{1}{24\Delta x}\left(\tilde{u}_i^n D_0^{(4)}\left[\tilde{u}_i^n\right] + \tilde{u}_i^{n+1} D_0^{(4)}\left[\tilde{u}_i^{n+1}\right]\right) \\ &+ \frac{\Delta t^2}{24}\left(D_{ttt}[\tilde{u}_i^n] + D_{ttt}[\tilde{u}_i^{n+1}]\right), \end{aligned} \tag{26}$$

where

$$D_{ttt}[\tilde{u}_i^n] = -\frac{1}{\Delta x^3}\left(6\tilde{u}_i^n (D_0^{(4)}[\tilde{u}_i^n])^3 + 9(\tilde{u}_i^n)^2 D_0^{(4)}[\tilde{u}_i^n] D_{xx}[\tilde{u}_i^n] + (\tilde{u}_i^n)^3 D_{xxx}[\tilde{u}_i^n]\right),$$

$D_{xx} = D_+ D_-(1 - D_+ D_-/12)$, and $D_{xxx} = D_0 D_+ D_-$.

Next we show how to determine $\tilde{e}_{i-1/2}^{n+1/2}$. A third-order estimate of the residual at time level $t = t^n$ is required. A Taylor series expansion about $t = t^n$ allows us to define

$$R_i^n = -\frac{\tilde{u}_i^{n+1} - \tilde{u}_i^n}{\Delta t} + \frac{\Delta t}{2\Delta x^2} D_{tt}[\tilde{u}_i^n] + \frac{\Delta t^2}{6\Delta x^3} D_{ttt}[\tilde{u}_i^n],$$

where $D_{ttt}[\tilde{u}_i^n]$ is as before and

$$D_{tt}[u_i^n] = 2u_i^n (D_0^{(4)}[u_i^n])^2 + (u_i^n)^2 D_{xx}[u_i^n].$$

From here it is straightforward to define left and right states for the Riemann problem using

$$\begin{aligned} \tilde{e}_{i,\pm}^{n+1/2} = \tilde{e}_i^n &+ \frac{1}{2}\left(\pm 1 - \frac{(\tilde{e}_i^n + \tilde{u}_i^n)\Delta t}{\Delta x}\right)\psi\left(D_+\left[\tilde{e}_i^n\right], D_+\left[\tilde{e}_{i-1}^n\right]\right) \\ &+ \frac{\Delta t}{2}\left(R_i^n - \frac{\tilde{e}_i^n}{\Delta x} D_0[\tilde{u}_i^n]\right). \end{aligned}$$

In addition, the primal approximation at the cell face is defined through Taylor expansion, for example as

$$\tilde{u}_{i-1/2}^{n+1/2} = \frac{\tilde{u}_i^n + \tilde{u}_{i-1}^n}{2}\left(1 - \frac{\Delta t}{\Delta x}(\tilde{u}_i^n - \tilde{u}_{i-1}^n)\right).$$

Finally, the Riemann problem at intercell interfaces is solved much as was done for the method-of-lines case (4.1.2) with all left and right values evaluated at the mid-time level.

5. Properties of the Nonlinear Error Transport Method

In this section, we demonstrate some properties of the proposed nonlinear error transport technique. We first consider the convergence properties of the error estimate for both smooth and discontinuous solutions for several discretizations. We then address a test problem from Zhang *et al.* [10] in order to compare and contrast several features of the methods.

5.1. Convergence Properties

Consider the sinusoidal initial value problem (IVP) for Burgers equation:

$$u(x, t = 0) = a - \sin(\pi x). \tag{27}$$

For times $t < t_b = \pi^{-1}$, the solution remains smooth and is implicitly given by

$$u(\xi, t) = a - \sin(\pi\xi)$$

along characteristics

$$x(\xi, t) = \xi + [a - \sin(\pi\xi)]t.$$

Regions of positive slope expand while regions of negative slope compress.

At $t = t_b$, shocks form at $x_s(t) = at + 2k$ for $k \in \mathbb{Z}$. For times $t \geq t_b$, the feet of the characteristics arriving at the shock at time t are $\xi_s(t)$, which are found by solving the transcendental equation

$$\xi_s(t) = t \sin(\pi\xi_s(t)).$$

The solution to Burgers' equation is then

$$u(x, t) = \begin{cases} a - \sin(\pi\xi), & |\xi| \geq |\xi_s(t)|, \\ a - \sin(\pi\xi_s(t)), & \text{otherwise}, \end{cases} \tag{28}$$

at locations corresponding to

$$x(\xi, t) = \begin{cases} \xi + [a - \sin(\pi\xi)]t, & |\xi| \geq |\xi_s(t)|, \\ x_s(t), & \text{otherwise}. \end{cases} \tag{29}$$

Each shock strength is

$$\left|u^+(x_s(t), t) - u^-(x_s(t), t)\right| = 2|\sin(\pi\xi_s(t))|. \tag{30}$$

The shocks grow in magnitude until $t = 1/2$, when the maxima of the solution catch the shocks, and the shocks catch the minima of the solution. After this time, the shocks decay.

We consider the convergence of the approximate error before and after the formation of discontinuities. In addition, the upwind differencing and potential slope limiting in our spatial discretization are both nonlinear switches that can reduce convergence rates in the primal approximation and estimated error.

5.2. Properties for Smooth Discretizations

In Section 2, we derived an upper bound for the convergence rate of the error given the orders of the primal operator, error operator, and residual operator discretizations. To satisfy the conditions that lead to that estimate, we consider the smooth solution (28) for $t < t_b$. Since the spatial discretizations of the primal and error operators in Section 4 were upwind-biased, these schemes will change if the solution is not positive or negative definite. We thus take $a = 2$ and consider the solution at time $t = 0.1$. In addition, we take ψ to be defined by (20b) in order to obtain a linear, formally second-order spatial discretization. The order relation (7) predicts that $|\tilde{e} - e| = O(\Delta x^4)$ for method-of-lines and space-time discretizations, since $p = q = 2$ and either residual evaluation (22) or (23) which both have r=4. As a result, the error estimate will be asymptotically correct in any L_p norm.

As a computational example, we simulate on the domain $x \in [-1, 1)$ using N points, apply periodic boundary conditions, and use a time step determined by a fixed CFL restriction of 0.9:

$$\max_{i \in [1,N]} (|\tilde{u}_i^n| + |\tilde{e}_i^n|) \frac{\Delta t}{\Delta x} \leq 0.9.$$

We consider a sequence of meshes $N \in \{10 \cdot 2^m; 2 \leq m \leq 9\}$ and perform convergence studies for both the method-of-lines and space-time schemes.

Figure 1 shows the results of the convergence study for the L_1 and L_∞ norms of the error in the approximate solution and the error in the approximate error at $t = 0.1$ for the method-of-lines scheme. The non-conservative form for the residual (22) was used. Here we can clearly see that second-order convergence is achieved for both norms of the approximate solution, and fourth-order convergence is achieved for both norms of the approximate

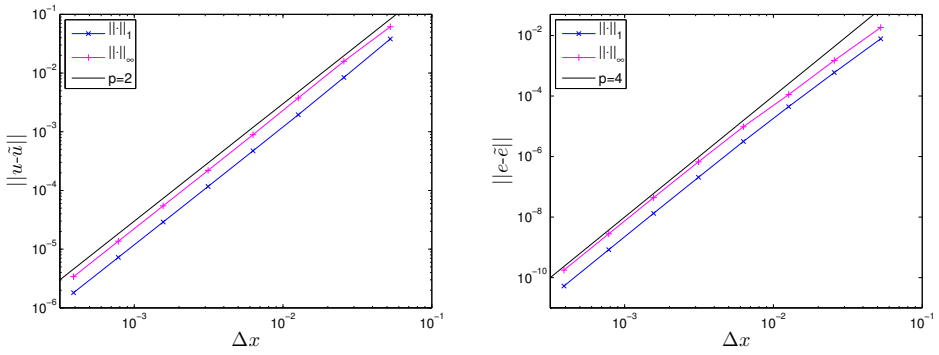

Figure 1: Convergence of the approximate solution and error at $t = 0.1$ for $u(x, t = 0) = 2 - \sin(\pi x)$ for the method-of-lines discretization of Burgers' equation.

error. This is a demonstration of the convergence rates as predicted by the order relation (7).

Similarly, Figure 2 shows the results of the same convergence study for the space-time formulation. Again, second-order convergence is achieved for both norms of the approximate solution, and fourth-order convergence is achieved for both norms of the approximate error as predicted by the order relation (7). For either scheme, the error estimate is asymptotically correct in any L_p norm.

5.2.1. Properties for Non-smooth Discretizations

In order to investigate the performance of the error estimation procedure when the upwind switch comes into play, we need only take $a = 0$ in our initial conditions (27). This causes the primal discretization to switch abruptly as the solution crosses through the origin at $x = 0$ and again at $x = \pm 1$. The result is that the error develops a kink or discontinuity at these points, and so the order relation (7) is no longer strictly applicable. Note that we simulate two periods for this case in order to more clearly display the effects of the upwind switch in Figure 4.

Figure 3 shows convergence study results for this case for the method-of-lines discretization using the non-conservative residual approximation (22). The primal approximate solution converges as expected at a second-order rate in both the L_1 and L_∞ error norms. However, while the L_1 error norm of the error still attains fourth-order convergence, the L_∞ error norm

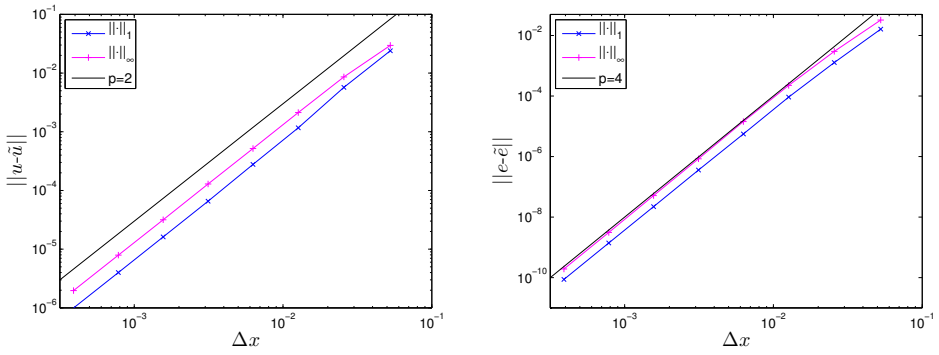

Figure 2: Convergence of the approximate solution and error at $t = 0.1$ for $u(x, t = 0) = 2 - \sin(\pi x)$ for the space-time discretization of Burgers' equation.

convergence is reduced to a third-order rate. In Figure 4, plots of the approximate solution and error show that the error field has singularities where the solution crosses through zero, *i.e.*, where the upwind scheme changes its stencil. Degraded convergence is well known in the presence of singularities [28]. We note that the error estimate is still asymptotically correct in any L_p-norm.

5.3. Error Evolution for Nonlinear Discretizations

From a practical perspective, one of the primary cases of interest is when nonlinear algorithms are used. These schemes experience nonlinearity from the equations as well as algorithmic nonlinearity from slope limiting. We would like to understand this important case and so we investigate the case where the reconstruction function is nonlinearly dependent on its arguments and take ψ to be defined by (20c). Both smooth and discontinuous solutions are of interest. One of the difficulties in this regime is that the use of the limiter can result in approximate solutions with degraded accuracy even when the exact solution is perfectly smooth. For instance, limiters like (20c) cannot distinguish between genuine and artificial extrema ($uv \leq 0$ in either case) and locally reduce to a low-order approximation for a small number of cells near the genuine extrema. This results in numerical errors that are not infinitely differentiable and has practical implications for the accuracy of the error evolution technique.

Take for example the initial condition (27) with $a = 1$. We consider the

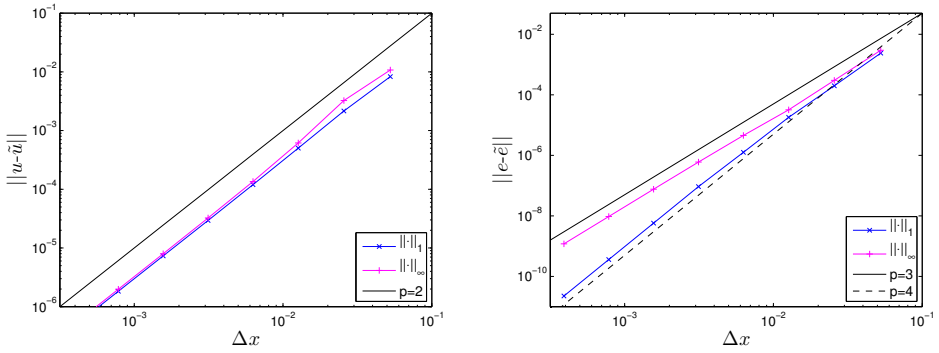

Figure 3: Convergence of the approximate solution and error at $t = 0.1$ for $u(x, t = 0) = -\sin(\pi x)$ for the method-of-lines discretization of Burgers' equation.

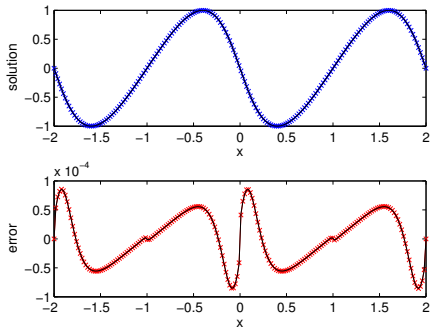

Figure 4: Plots of the approximate solution and error at $t = 0.1$ and $N = 200$ points for initial data $u(x, t = 0) = -\sin(\pi x)$ for the method-of-lines discretization of Burgers' equation. The exact solution and exact error are indicated by black lines, while the marks indicate the approximate results.

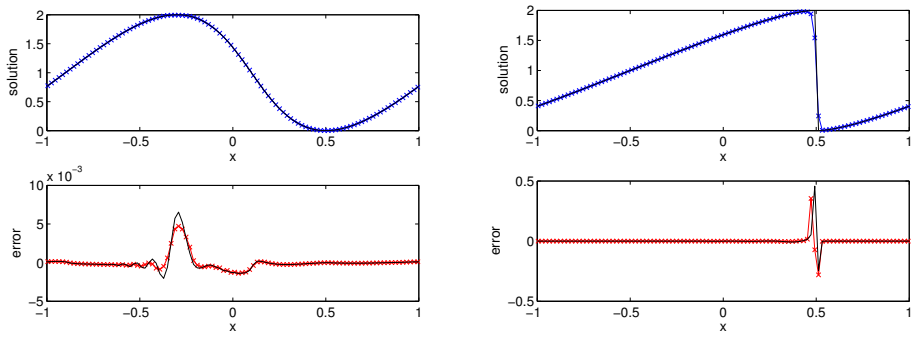

Figure 5: Solution and error of the Burgers' equation for initial data $u(x, t = 0) = 1 - \sin(\pi x)$ at $t = 0.1$ (left) and $t = 0.5$ (right). The method-of-lines scheme with the MinMod limiter was used for both the primary and error evolution equations on a grid of $N = 100$ points in $x \in [-1, 1)$. The non-conservative residual approximation was used. Black lines indicate exact values while marks indicate discrete approximations.

method-of-lines formulation with the non-conservative residual approximation; results for the space-time scheme are similar. In Figure 5, the discrete approximation and approximate error using $N = 100$ points for $x \in [-1, 1)$ are shown at a time when the exact solution is smooth ($t = 0.1$) as well as after a shock has formed ($t = 0.5$). Prior to shock formation, the main feature present in the error is the peak associated with extrema clipping at the maximum value; note that a similar error does not occur at minima since the solution value is zero at that point. The error approximation captures this feature quite well and even captures some small oscillations after this peak. After shock formation, the error is almost entirely dominated by $O(1)$ error near the captured numerical shock. The approximate numerical error represents this feature remarkably well but the large variation over a small number of cells causes some difficulty in representing details of the error through the shock.

The asymptotic convergence rates of the various approximations are also interesting. Figure 6 shows the results of a convergence study for the approximate solution. Prior to shock formation, the error behaves largely as it would for a TVD scheme applied to linear advection of a smooth profile. The large error introduced near the extrema impacts the L_∞ error norm most, and we see convergence rates that trend towards a value of $4/3$. Interestingly, this is the expected rate of convergence near a slope discontinuity for a second

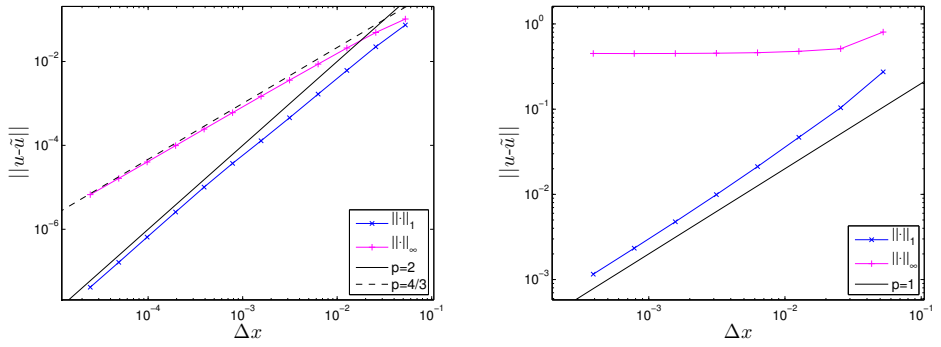

Figure 6: Approximate solution convergence for Burgers equation with initial data $u(x, t = 0) = 1 - \sin(\pi x)$ at $t = 0.1$, before shock formation (left), and at $t = 0.5$, after shock formation (right). The method-of-lines discretization and the MinMod limiter was used for both the primal and error equations. The non-conservative residual approximation was used.

order scheme [28]. The L_1 error norm is less sensitive and asymptotically tends to the rate of two. Note that other p-norms with $1 < p < \infty$ will exhibit convergence rates between these two extremes. After the formation of a shock in the flow, the L_∞ error norm is no longer convergent, which is to be expected because of the point-wise $O(1)$ error in the neighborhood of the captured shock. On the other hand, the L_1 error norm converges at the expected first-order rate.

The asymptotic behavior of the approximate error is less clear, as is shown in Figure 7. For smooth flows, the L_∞ error norm of the error is again seen to converge near the $4/3$ rate that was seen for the approximate solution, but very high resolution ($N > 20000$) is needed to achieve this. Likewise, L_1 convergence rate of the approximate error approaches the second-order rate as seen for the approximate solution, but only for very high spatial resolutions. After shock formation, the picture is again much clearer as the L_1 convergence of the approximate error exhibits first-order convergence while the L_∞ error norm does not converge.

Since the errors in the approximate solution and approximate error are converging at the same rates, the error estimate is not asymptotically correct in any L_p norm. Of course, the fidelity of the approximate solutions shown in Figure 6 suggest that the estimated error can still be useful. For instance, p-norm convergence of the error estimate on sub-domains is found to be

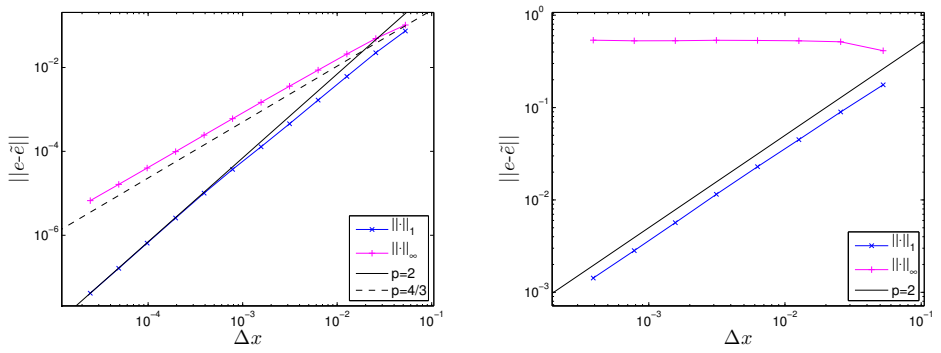

Figure 7: Approximate error convergence for Burgers equation with initial data $u(x, t = 0) = 1 - \sin(\pi x)$ at $t = 0.1$, before shock formation (left), and at $t = 0.5$, after shock formation (right). The method-of-lines discretization and the MinMod limiter was used for both the primal and error equations. The non-conservative residual approximation was used.

asymptotically correct for many cases. Preliminary work also indicates that error estimates for a large class of quantities of interest constructed from the error field are asymptotically correct. These will be the subject of future work. Finally, we note that these results are robust for any choice of the offset a in the initial condition. This implies that the role of the nonlinear limiters is in some sense more important than the role of nonlinearities from upwind switching. This is at least partly the result of the fact that the solution is close to zero when the upwind direction switches. In contrast the solution can be any size near characteristic extrema which cause algorithm switches.

5.4. The Effects of Error Nonlinearity

In the existing literature, the error equation operator is always linearized. For Burgers' equation, the corresponding linear error transport equation is

$$\partial_t e + \partial_x (\tilde{u} e) \approx -\partial_t \tilde{u} - \partial_x \left(\frac{1}{2} \tilde{u}^2 \right). \tag{31}$$

The justification for applying (31) is that the $e\partial_x e$ term is higher-order and is thus negligible. Hay and Visonneau [16] investigate eliminating the $e\partial_x \tilde{u}$ term as well and determine that they do not obtain an asymptotically correct error estimate unless they use the form (31). However, even this form is not consistent with the original nonlinear error equation and cannot produce

asymptotically correct results if e is large. Errors may not be small if the primal scheme is of low-order, if singularities exist in the solution, if very long-time integrations are sought, if solution features are under-resolved, or possibly other scenarios. If one can handle numerically the nonlinearity of the primal equation, one should be able to handle the nonlinearity in the error equation. Our conjecture is that solving the fully nonlinear error equation will make the error estimates more robust. We demonstrate differences between linear and nonlinear error transport using two canonical cases for the simple problem of the inviscid Burgers' equation.

5.4.1. Low-Order Approximations

One case where ignoring error nonlinearity produces unsatisfactory results is when a low-order forward approximation is used but the approximate error is sought to higher accuracy. This, for example, was done in [10]. We define the primal scheme using the ψ defined by (20a) and the error transport scheme using the ψ defined by (20b). Thus, the forward approximation is the first-order upwind method, while the error approximation uses the second-order upwind method. For this case, we show the convergence of the error approximations using the linearized equation (31) as well as the fully nonlinear error equation (17). A conservative numerical approximation to (31) is easily defined as before, but the solution to the Riemann problem requires only the sign of the face values $\tilde{u}_{i\pm1/2}$. The method-of-lines formulation with non-conservative residual approximation is used for both equations.

Under the same assumptions originally used to derive the order relation (7), neglecting the $e\partial_x e$ term is akin to making an additional $O(e^2) = O(\Delta x^{2p})$ error. Thus, the order relation for the linear error transport is

$$|\tilde{e} - e| = O\big(\Delta x^{\min(2p,p+q,r)}\big)\,. \tag{32}$$

For $p = 1$, $q = 2$, and $r = 4$, we therefore expect second-order convergence for the linear error transport method and third-order convergence for the nonlinear error transport method. Results of a convergence test for the initial condition (27) with $a = 2$ at time $t = 0.1$ are presented in Figure 8. It is clear that the effect of neglecting the nonlinear term is to reduce the order of the error approximation from third to second order in both L_1 and L_∞ norms. Notice that by leaving out the $e\partial_x e$, one is limited to second order accuracy. One can, in principle, obtain arbitrary accuracy with its inclusion.

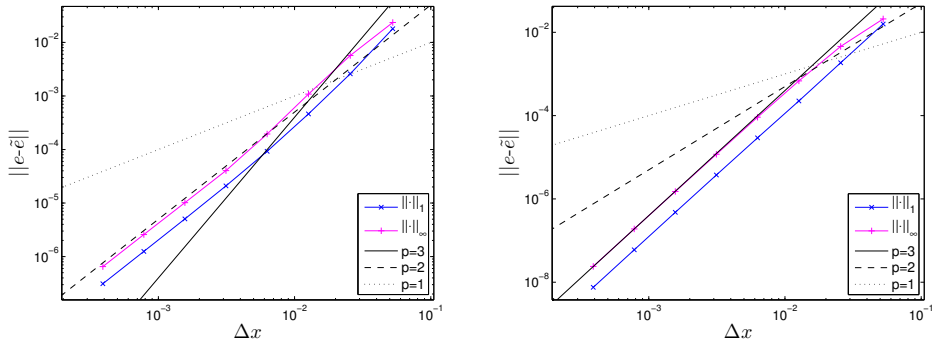

Figure 8: Convergence of the approximate solution and error at $t = 0.1$ for $u(x, t = 0) = 2 - \sin(\pi x)$ for the Burgers' equation using a method-of-lines discretization. The primal operator spatial discretization is first-order, while the error operator spatial discretization is second-order. At left are results found using the linearized equation (31), while at right are results found using the fully nonlinear error equation (17).

5.4.2. Regions of Large Error

Error nonlinearity is also important when the solution develops non-differentiable features. For cases where a shock is captured, the numerical error is as large as the solution itself, and so nonlinear error effects are equally important as the pure linear transport of error. To illustrate this point we again use the initial condition (27) with $a = 0$ and consider the solution at time $t = 0.5$, after a shock forms. The schemes are defined using the ψ defined by (20b), which leads to unlimited, second-order upwind discretizations.

As before, the convergence study results shown in Figure 9 reveal that the L_1 error norm of the primal solution is converging at a first-order rate while the L_∞ error norm is non-convergent. The plots of the convergence character for the approximate error are more interesting. When the linearized error transport operator of (31) is used, the error is divergent in the L_∞ error norm and not convergent in the L_1 error norm. On the other hand, the approximate error found using the nonlinear error evolution operator of (17) converges at a first-order rate in the L_1 error norm and is non-convergent in the L_∞ norm. For the linear error transport equation, the error at the stationary shock grows with time because the residual continues to drive the error equation at the shock, but the linear transport operator is unable to transport this error away and obtain a steady state. In essence, the linear

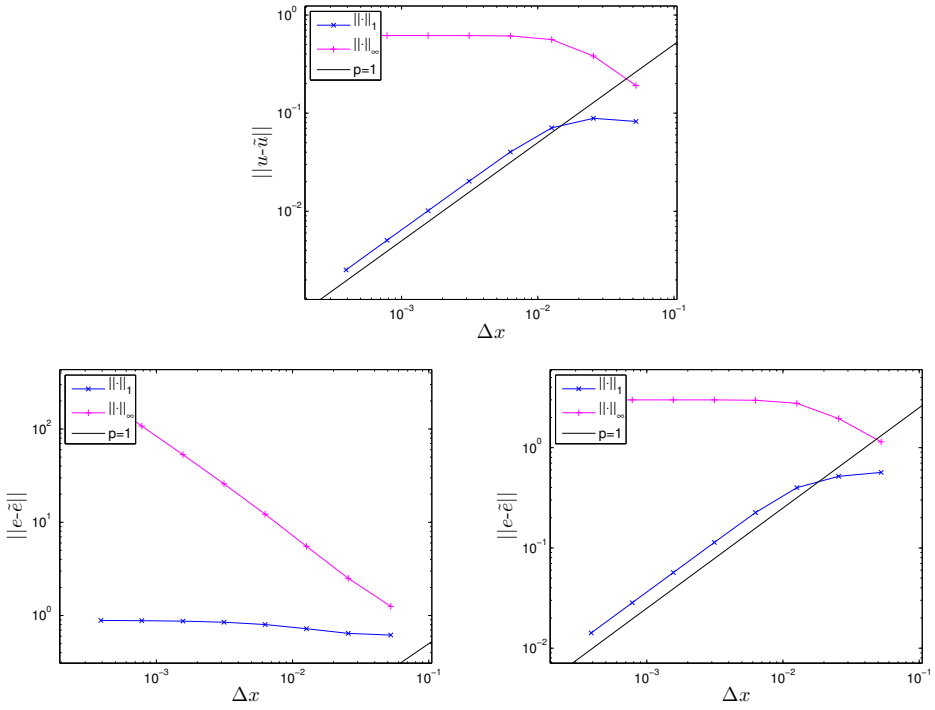

Figure 9: Convergence of the approximate solution (top), approximate error using linear error transport (bottom left), and approximate error using nonlinear error evolution. All results are presented at $t = 0.5$ for Burgers' equation with initial data $u(x, t = 0) = -\sin(\pi x)$.

error transport equation can be unstable at a shock. The nonlinear advection term in the nonlinear error transport equation, on the other hand, provides a mechanism to move error into the shock where it is destroyed by cancellation.

We note that this result is dependent on the shock being stationary (or slowly moving) and that it does not always appear, depending on the location of the shock relative to discretization points. Additional concerns relative to the choice of quasi-linear vs. conservative residual approximation, method-of-lines vs. space-time discretization, and others can effect the presence or nature of the instability. Some of these choices are addressed in Section 5.5. Nevertheless, it is a matter of concern for the linear error transport approach that instability can result for some discretization choices, while these difficulties are easily forestalled by solving the fully consistent nonlinear error transport equation.

5.5. Comparisons for the Problem of Yang and Przekwas

A discontinuous IVP used by Zhang *et al.* [10] is the problem of Yang and Przekwas [29]. For comparison purposes, we consider this IVP as well. We will demonstrate that the particular discretization of the residual in [10] preserves certain properties of the governing equation that may motivate the use of conservative residual evaluations. We address their results within the context of our own and make a point about quality of the error relative to the order of the primal discretization.

Consider the compactly-supported IVP for Burgers equation:

$$u(x,t=0) = \begin{cases} 1, & 1/5 < x < 2, \\ -1/2, & 2 < x < 3, \\ -1, & 3 < x < 24/5, \\ 0, & \text{otherwise.} \end{cases} \tag{33}$$

For times $t < 1$, the solution is

$$u(x,t) = \begin{cases} (5x-1)/(5t), & 1/5 < x < 1/5 + t, \\ 1, & 1/5 + t < x < 2 + t/4, \\ -1/2, & 2 + t/4 < x < 3 - 3t/4, \\ -1, & 3 - 3t/4 < x < 24/5 - t, \\ (5x-24)/(5t), & 24/5 - t < x < 24/5, \\ 0, & \text{otherwise.} \end{cases} \tag{34}$$

At $t = 1$, the two initial shocks collide, resulting in a stationary shock at $x = 9/4$. For times $1 \leq t < 41/20$, the solution is

$$u(x,t) = \begin{cases} (5x-1)/(5t), & 1/5 < x < 1/5 + t, \\ 1, & 1/5 + t < x < 9/4, \\ -1, & 9/4 < x < 24/5 - t, \\ (5x-24)/(5t), & 24/5 - t < x < 24/5, \\ 0, & \text{otherwise.} \end{cases} \tag{35}$$

At $t = 41/20$, the left expansion fan encounters the shock, and the shock weakens and begins to move to the left.

5.5.1. Conservative versus Non-Conservative Residual Evaluation

Zhang *et al.* [10] present results to the Yang and Przekwas problem in Figures 3 through 6 of their paper at times $t = \{0.5, 1.0, 1.5, 2.0\}$. They used a first-order upwind finite volume scheme for the primal solution and both first-order and high-resolution finite volume schemes for their linear error transport equation. Their source term evaluation used the leading-order truncation error terms evaluated using limited conservative flux differencing.

These results have some interesting features. In all their figures, spikes occur in the computed error at the stationary ends of the expansion fans ($x = 0.2, 4.8$). In addition, the error in the propagating shocks, which merge into a stationary shock at $t = 1.0$, virtually disappears in the $t = 1.5$ results. Of course, the exact error does vanish in this case, because the Riemann solver that they use has the property that the jump across a stationary shock at a cell interface is exact. Nevertheless, these results raised some questions, such as the cause of the spikes at the ends of the expansion fans and the mechanism by which the error at the shock vanished.

As discussed in Section 5.4.2, one expects an advantage of nonlinear error transport over linear error transport to occur where errors are large relative to the solution. Two such locations in this problem are at the shock(s) and where the solution vanishes but the error does not, *i.e.*, at the fixed end of the expansion fans. The linear transport operator provides no means for the error field to expand or compress independently of the primal solution. The nonlinear error operator, on the other hand, allows for these nonlinear effects. Thus, one would expect errors transported nonlinearly to steepen at a shock, or specifically, be advected into and destroyed by a stationary shock in the

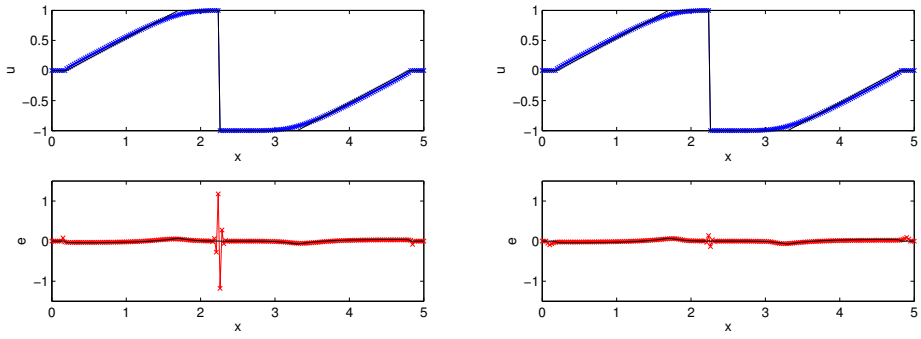

Figure 10: Solution and error at time $t = 1.5$ for (left) linear error transport and (right) nonlinear error transport using conservative residual evaluation. Results computed with $N = 200$ points. The primal solution is first-order and the error discretization is second-order.

scalar case. A linear transport operator cannot move errors into a stationary shock; numerical errors should be accumulated in the two cells adjacent to a stationary, face-aligned shock.

Thus, the disappearance of error at the stationary shock between Figures 4 and 5 of [10] is puzzling. The only other obvious mechanism by which error can be destroyed is for the residual to act as a sink. However, at a stationary, face-aligned shock, the residual of the form of Equation (16) in [10] vanishes. Using both finite-volume and finite-difference variants based on our understanding of the scheme in [10], which is not unambiguous, we have been unable to reproduce these results. Instead, we obtain finite errors in the two cells neighboring the shock that neither grow nor decay. In contrast, using nonlinear transport, we see that the errors at the shock decay. An example using our finite-difference approach with a conservative residual evaluation is presented in Figure 10.

In Section 5.4.2, the error at a stationary shock as computed using linear transport grew in time, while that is not case in Figure 10. The difference is in the evaluation of the residual: in the former, the quasi-linear form (22) was used whereas in the latter, the conservative form (23) was used. While the conservative approximation is formally less accurate, the residual evaluation vanishes for stationary shocks aligned with the mesh. Thus, for linear error transport, errors near stationary shocks may not grow. To illustrate this fact further, the maximum of the exact and approximate errors as functions of

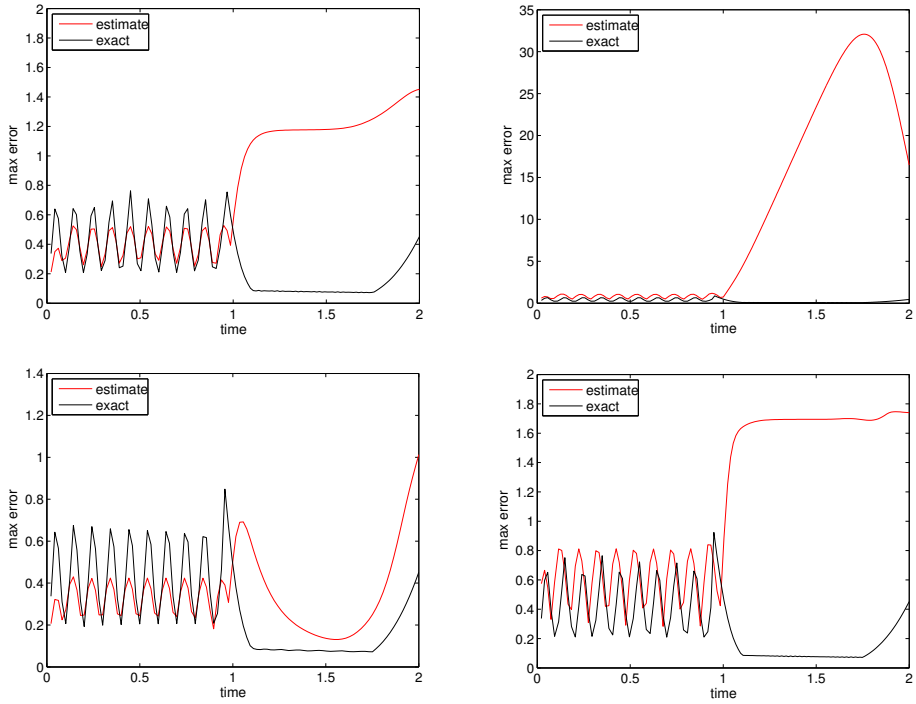

Figure 11: Maximum of error and estimated error as functions of time for $N = 200$ points. At top is linear transport and at bottom is nonlinear evolution. At left is conservative and at right is quasi-linear residual evaluation. The primal solution is first-order and the error discretization is second-order.

time for $N = 200$ points using linear transport, nonlinear evolution, and both quasi-linear and conservative evaluations of the residual are plotted in Figure 11. For the combination of linear transport and quasi-linear residual approximation, blowup of the solution is seen (note the scale), as was the case in Section 5.4.2. The eventual decay of the maximum estimated error is the result of the numerical rarefaction interaction with the shock, which occurs earlier than the exact solution due to numerical diffusion. On the other hand, the conservative residual approximation shows no such blowup for linear or nonlinear error transport methods. The oscillations in the error before $t = 1$ are the result of the approximate representation of the slower right-moving shock as it traverses cells; the period is roughly 0.1, which would give a speed of 0.25 on a mesh of size $\Delta x = 0.025$. It is also interesting to note that

the conservative residual schemes appear to have better phase agreement and that for the quasi-linear residual schemes, the linear transport phase agreement gets increasingly worse, whereas the nonlinear transport phase agreement appears to lock into a fixed phase shift.

For completeness, we comment that the initial location and treatment of the discontinuities matters for these results. For $N = 200$ points with a conservative finite-difference scheme, there is no ambiguity in the initial condition taken as point-wise values. For $N = 201$, initial discontinuities occur at nodes; if the mid-value of the jump is used as the initial condition, no growth is seen in the error at the shock for linear transport. For results obtained with $N = 201$ points, we take this definition.

Figure 12 shows the approximate solution and error along with the exact solution at $t = 0.5$. Results are presented for linear and nonlinear transport using conservative and quasi-linear evaluation of the residual. Several features merit discussion. In all cases, the error at the slowly right-moving shock is not as well represented as the faster left-moving shock. For the errors at the shocks, the steepening of the error for the nonlinear transport results is apparent when compared to the linear transport results. In contrast, the linear transport results produce expansions that have slightly less phase error than the nonlinear transport results. Finally, the spikes that occur at the stationary ends of the expansions in [10] occur for the conservative evaluation of the residual, but not significantly for the quasi-linear evaluation. We cannot at this time adequately explain these latter two results.

5.5.2. On the Error of Higher-Order Schemes

One very important fact to realize is that, by (32), the error shown in Figure 12 for linear transport is at most second-order accurate while the error for nonlinear transport is up to third-order accurate for smooth enough portions of the flow, as discussed in Section 5.4.1. This is an interesting point because, asymptotically, there is no benefit to using a second-order accurate evaluation of the linear transport operator because no asymptotic gain is found over a first order solution. What then do the error estimates look like for higher-order or, even more interestingly, for TVD, limited discretizations? Figure 13 shows results when the TVD limited scheme is used for the primal solution and the second-order unlimited scheme is used for the error. Even though there is visually very little difference between the primal approximation when compared to Figure 12, the quality of the error approximation is

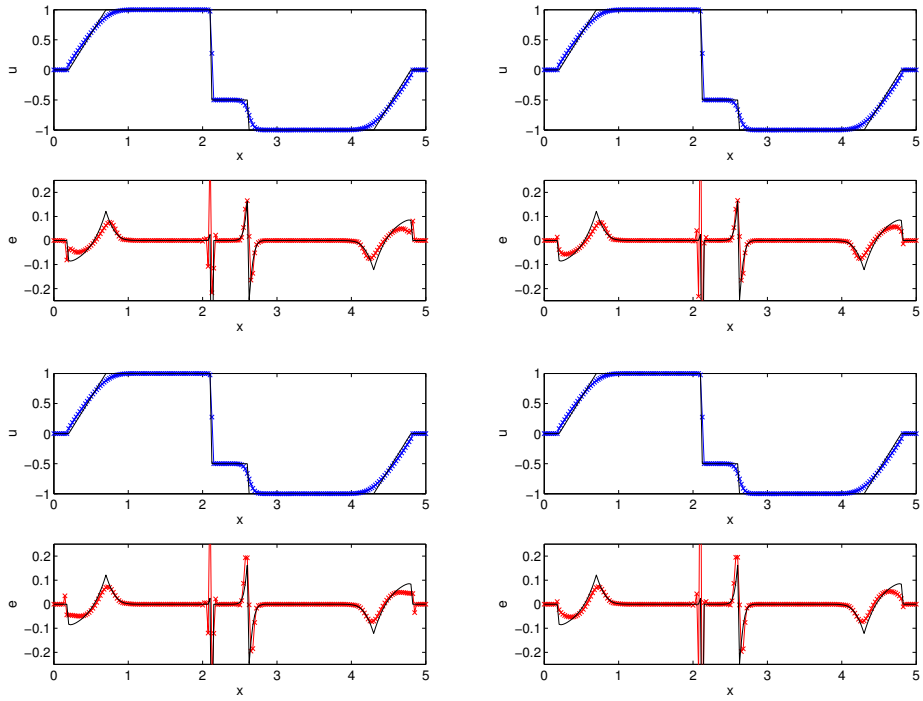

Figure 12: Zhang test problem at $t = 0.5$ with $N = 201$ points using first-order primal and second-order error discretizations. At top is nonlinear transport using conservative (left) and quasi-linear (right) evaluation of residual. At bottom is linear transport with conservative (left) and quasi-linear (right) evaluation of residual. Note that quasi-linear residual with linear transport can be unstable and so is not recommended.

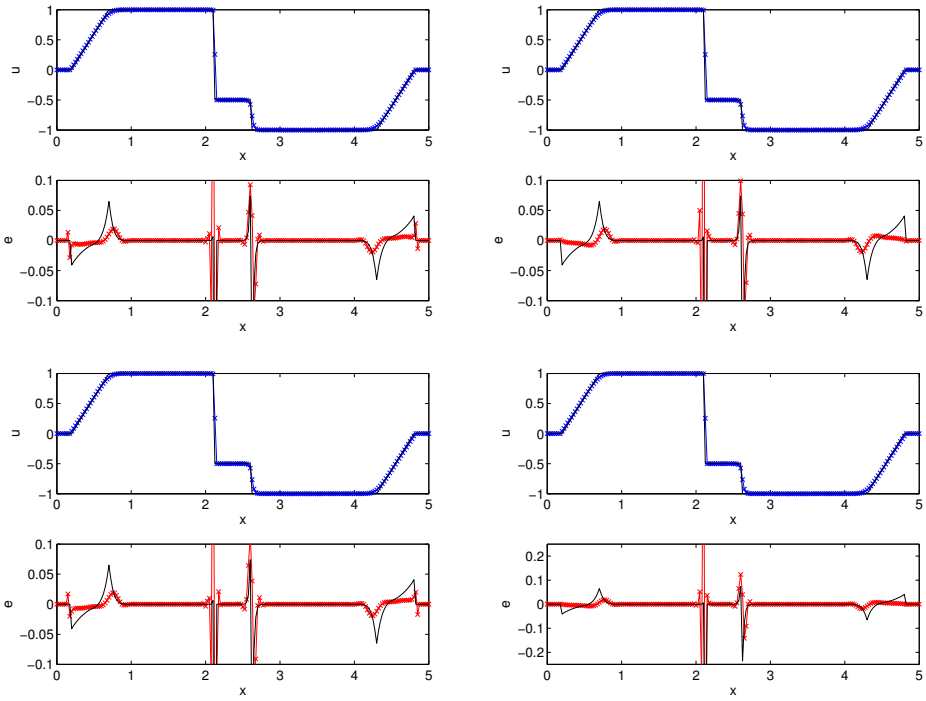

Figure 13: Zhang test problem at $t = 0.5$ with $N = 201$ points using second order primal and second order error discretizations. At top is nonlinear evolution using conservative (left) and quasi-linear (right) evaluation of residual. At bottom is linear transport with conservative (left) and quasi-linear (right) evaluation of residual. Note that quasi-linear residual with linear transport can be unstable and so is not recommended.

worse in all cases. Practically, this combination of schemes is the most realistic situation for a problem of this type, and so it is discouraging to see the difficulties presented for error transport. Based on our albeit limited experience, this result appears to be a worst-case scenario that correlates with the discontinuous initial conditions for this scalar equation. We generally obtain better results when sharp flow features develop naturally in the flow, as seen in Section 5.3, or for systems, as will be demonstrated in the next section.

6. Application to the Euler Equations

We have thus far limited out application to a scalar nonlinear hyperbolic equation. In this section, we briefly consider the one-dimensional ideal gas Euler equations of fluid dynamics, which represent a hyperbolic system of nonlinear equations. While treating a system with the error evolution approach is no different *per se*, we do note that the Burgers' equation possesses a particularly amenable nonlinearity; its quadratic form produces a particularly simple form of $\mathcal{G}(\tilde{e};\tilde{u})$ in the nonlinear error equation (4).

In contrast, the Euler equations for even simple ideal gas also contain cubic or inverse nonlinearities. Obvious approaches to evaluate $\mathcal{G}(\tilde{e};\tilde{u})$ can lead to violations of auxiliary constraints, such as the positivity of mass density or pressure. We will show that a simple solution to this problem is to work in a flux-divergence form but to use an approximate Riemann solver based solely on the approximate primal solution.

The one-dimensional Euler equations are a system of conservation laws of the form (11) with state vector $u = (\rho, \rho v, \rho E)$ and flux vector $f(u) = (\rho v, \rho v^2 + p, \rho v H)$. Here, ρ is the mass density; v is the velocity; p is the pressure; $E = e + v^2/2$ is the total specific energy; and $H = E + p/\rho$ is the total specific enthalpy. The ideal equation of state $p = (\gamma - 1)\rho e$ is used to close the system of equations.

6.1. Discretization

For simplicity, we will use a method-of-lines approach. As in Section 4.1, we use a conservative discretization for the primal equation with an exact Riemann solver (See, *e.g.*, Toro [26]) and limited piecewise-linear reconstruction with the minmod limiter (20c). This results in a primal approximation of the form

$$\partial_t \tilde{u}_i = -\frac{1}{\Delta x} D_+ \left[f(\tilde{u}_{i-1/2}) \right].$$

As previously for Burgers' equation, the semi-discrete approximation of the error equation is

$$\partial_t \tilde{e}_i = -\frac{1}{\Delta x} D_+ \left[f(\tilde{u}_{i-1/2} + \tilde{e}_{i-1/2}) - f(\tilde{u}_{i-1/2}) \right] - \mathcal{R}(\tilde{u}_i) \tag{36}$$

The primary question then becomes the evaluation of the discrete flux $f(\tilde{u}_{i-1/2}+\tilde{e}_{i-1/2}) - f(\tilde{u}_{i-1/2})$. Therefore, assume a face value $\tilde{u}_{i-1/2}$ given by continuous polynomial interpolation, and left and right states $e_{i-1,+}$ and $e_{i,-}$ given by limited piecewise liner reconstruction are known. Determine the eigendecomposition $R\Lambda R^{-1} = \partial_u f(\tilde{u}_{i-1/2})$. Notice that by using the state $\tilde{u}_{i-1/2}$ rather than averages of the primal solution and face approximations of the error, the possibility of negative densities, pressures, or other unphysical states is eliminated. We now compute characteristic quantities $w_{i-1,+} = R^{-1} e_{i-1,+}$ and $w_{i,-} = R^{-1} e_{i,-}$ and compute the solution to the Riemann problem as

$$w^{(k)}_{i-1/2} = \begin{cases} w^{(k)}_{i-1,+} & \text{if} \quad \Lambda^{(k,k)} > 0 \\ w^{(k)}_{i,-} & \text{else} \end{cases}$$

for $k = 1, 2, 3$. Here the superscripts (k), or (k,k) indicate entries in the vector or matrix respectively. Finally we compute the face solution as $\tilde{e}_{i-1/2} = R w_{i-1/2}$ which completes the description. We note that this procedure amounts to a particular choice of linearized Riemann solver, but by using (36), the full nonlinear evolution of the error is retained. Finally, we note that a conservative, fourth-order approximation of the residual is employed.

6.2. Application

For a demonstration, we consider a shock-tube IVP problem on $x \in \mathbb{R}$ with piecewise-constant initial data:

$$u = \begin{cases} u_L, & x < 1/2, \\ u_R, & x > 1/2. \end{cases} \tag{37}$$

We define the left and right states in primitive variables to be $(\rho_L, v_L, p_L) = (1, 0, 1)$ and $(\rho_R, v_R, p_R) = (0.125, 0, 0.1)$, which defines the standard Sod problem. The exact solution, which consists of a leftward-traveling expansion fan, a slow rightward-traveling contact discontinuity, and a faster rightward-traveling shock, can be found in [26].

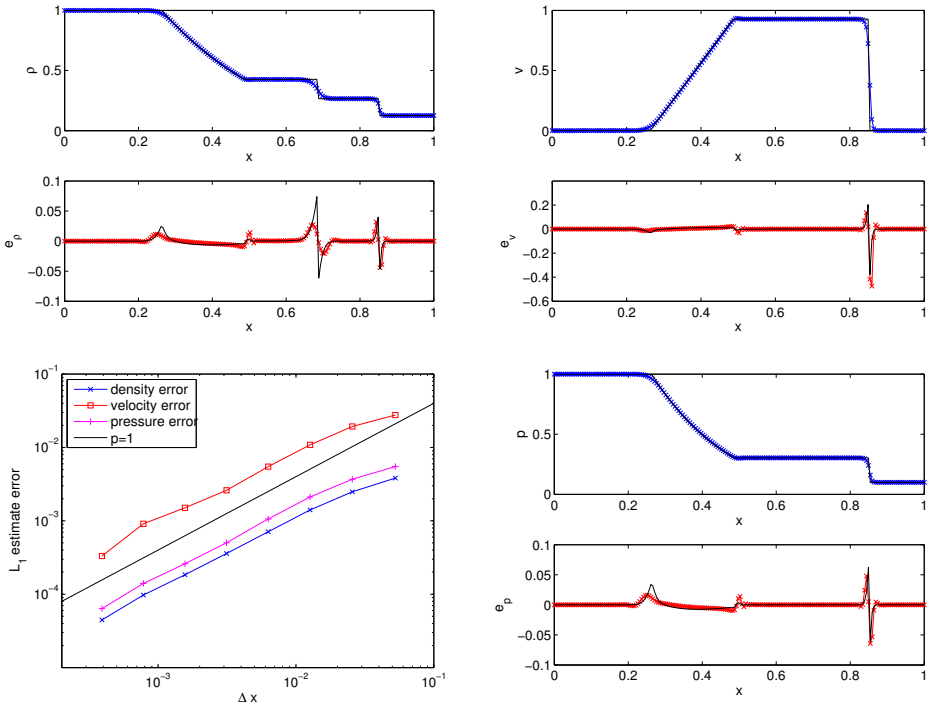

Figure 14: Approximation at time $t = 0.5$ for Sod's shock-tube problem using nonlinear error transport. Here second-order TVD algorithms have been used for spatial discretization of both primal and error equations and RK-4 for time integration. Clockwise from top left are the density, velocity, pressure, and estimated error convergence study.

We simulate on the domain $x \in [0, 1]$ until the time $t = 0.5$ so as to prevent the waves in the solution from reaching the domain boundaries. Thus, we exactly specify the boundary conditions using the piecewise constant initial data. We use the standard mesh of 200 points and plot results for a fixed CFL number of 0.4, which has no particular significance.

The results, shown in Figure 14, are quite similar to those obtained for the inviscid Burgers' equation. In this case, the error in the shock is captured very well, and the corners of the expansion fan have roughly the same degree of fidelity as seen for Burgers'. The contact discontinuity in the density field is the source of dominant error in the density field, and since this is a linearly degenerate wave with no self-steepening mechanism, capturing schemes will always smear out this wave. We see that the nonlinear error transport scheme

does as well as could be expected in representing the sharp feature in the error at the contact. We also present a convergence study for the L_1 errors in the estimated errors. Near first order convergence is demonstrated for the grid resolutions presented. These results demonstrate that the nonlinear error transport approach generalizes to nonlinear systems with more complicated nonlinearities than that in Burgers' equation.

7. Conclusions

In this paper, we have investigated the nonlinear error transport method as a technique to estimate the discretization error for finite volume and finite difference discretizations of nonlinear hyperbolic equations. We used the scalar, time-dependent inviscid Burgers' equation as a canonical model and considered both continuous and discontinuous solutions. In contrast to prior linear transport approaches, our technique is novel because we preserved the nonlinear terms in the error equation and used a direct, systematic approach to the discretization of the error residual operator that does not require knowledge of the modified differential equation of the discretization of the primal equation. We demonstrated the approach for both method-of-lines and space-time formulations, considered linear and nonlinear discretizations and compared conservative and quasi-linear residual discretizations. Finally, the method was applied to the unsteady Euler equations in one spatial dimension, which provided a demonstration of an approach to handling more complicated nonlinearities.

Our results demonstrate that, on the whole, the method is a reasonable approach. For strong solutions, the results are in excellent agreement with the asymptotic theory. Nonlinear schemes and weak solution features such as solution and slope discontinuities degrade the convergence of the error estimates. From a point-wise perspective, the computed error occurs generally in the correct location, but the magnitudes will be incorrect in the vicinity of weak solution features. This later behavior is exacerbated by a higher-order primal solution and requires further investigation.

For problems involving shocks, there appears to be an advantage to using a conservative residual evaluation. In contrast to linear transport, numerical experiments suggest that, when properly formulated, nonlinear error transport can provide bounded estimates of error, whereas linear transport schemes may allow for unbounded growth in the error near a shock. In addition, the linear transport approach formally can produce a lower-order error

estimate even in smooth regions of the solution. For these reasons, we advocate using the fully nonlinear error transport equation with a conservative residual discretization, particularly for problems with weak solutions.

Beyond further investigation of the limitations of nonlinear error transport for weak solutions computed with higher-order primal schemes, there are several other directions we will consider in future work. The inclusion of non-periodic boundary conditions and extension to multiple dimensions should be straight-forward. Incorporating operator and dimensional splitting is another issue for investigation. In addition, coupling different primal models across domain boundaries is a logical extension of these techniques. Further developments will be sought for theoretical bounds on the amplitude errors for different weak solution features and understanding the asymptotic nature of errors in quantities of interest constructed from computed error fields.

References

[1] R. D. Skeel, Thirteen ways to estimate global error, Numer. Math. 48 (1986) 1–20.

[2] P. J. Roache, Verification and Validation in Computational Science and Engineering, Hermosa Publishers, Albuquerque, NM, 1998.

[3] L. F. Richardson, The deferred approach to the limit. Part I. Single lattice, Tansactions of the Royal Society of London, Series A 226 (1927) 299–361.

[4] F. M. Hemez, J. S. Brock, J. R. Kamm, Non-linear Error Ansatz Models in Space and Time for Solution Verification, AIAA Paper 2006-1995, 2006.

[5] M. Ainsworth, J. T. Oden, A posteriori error estimation in finite element analysis, Comput. Method Appl. M. 142 (1997) 1–88.

[6] M. B. Giles, E. Süli, Adjoint methods for PDEs: *a posteriori* error analysis and postprocessing by duality, Acta Numerica 11 (2002) 145–236.

[7] D. Estep, M. Larson, R. Williams, Estimating the error of numerical solutions of systems of nonlinear reation-diffusion equations, Mem. Am. Math. Soc. 696 (2000) 1–109.

[8] I. Babuška, T. Strouboulis, C. S. Upadhyay, A model study of the quality of a posteriori error estimators for linear elliptic problems. Error estimation in the interior of patchwise uniform grids of triangles, Comput. Method Appl. M. 114 (1994) 307–378.

[9] H. J. Stetter, The defect correction principle and discretization methods, Numer. Math. 29 (1978) 425–443.

[10] X. D. Zhang, J.-Y. Trépanier, R. Camarero, A posteriori error estimation for finite-volume solutions of hyperbolic conservation laws, Comput. Method Appl. M. 185 (2000) 1–19.

[11] Y. Qin, T. I.-P. Shih, A Method for Estimating Grid-Induced Errors in Finite-Difference and Finite-Volume Methods, AIAA Paper 2003-0845, 2003.

[12] B. van Straalen, A Posteriori Error Estimation for Finite Volume Simulations of Fluid Flows, Master's thesis, University of Waterloo, 1996.

[13] Y. Qin, T. I.-P. Shih, A Discrete Transport Equation for Error Estimation in CFD, AIAA Paper 2002-0906, 2002.

[14] Y. Qin, T. I.-P. Shih, Analysis and Modeling of the Residual in Discrete-Error-Transport Equation, AIAA Paper 2003-3850, 2003.

[15] I. Celik, G. Hu, Single grid error estimation using error transport equation, J. Fluid Eng.-T. ASME 126 (2004) 778–790.

[16] A. Hay, M. Visonneau, Error estimation using the error transport equation for finite-volume methods and arbitrary meshes, Int. J. Comput. Fluid D. 20 (2006) 463–479.

[17] C. Ilinca, X. D. Zhang, J.-Y. Trépanier, R. Camarero, A comparison of three error estimation techniques for finite-volume solutions of compressible flows, Comput. Method Appl. M. 189 (2000) 1277–1294.

[18] Y. Qin, P. S. Keller, R. L. Sun, E. C. Hernandez, C.-Y. Perng, N. Trigui, Z. Han, F. Z. Shen, T. Shieh, T. I.-P. Shih, Estimating Grid-Induced Errors in CFD by Discrete-Error-Transport Equations, AIAA Paper 2004-656, 2004.

[19] N. A. Pierce, M. B. Giles, Adjoint and Defect Error Bounding and Correction for Functional Estimates, AIAA Paper 2003-3846, 2003.

[20] N. A. Pierce, M. G. Giles, Adjoint and defect error bounding and correction for functional estimates, J. Comput. Phys. 200 (2004) 769–794.

[21] A. Jameson, W. Schmidt, E. L. Turkel, Numerical Simulation of the Euler Equations by Finite Volume Methods Using Runge-Kutta Time Stepping Schemes, AIAA Paper 81-1259, 1981.

[22] P. Lax, B. Wendroff, Systems of conservation laws, Comm. Pure Appl. Math. 13 (1960) 217–237.

[23] B. van Leer, Towards the ultimate conservative difference scheme, V. A second-order sequel to Godunov's method, J. Comput. Phys. 32 (1979) 101–136.

[24] B. van Leer, On the relation between the upwind-differencing schemes of Godunov, Engquist-Osher and Roe, SIAM J. Sci. Statist. Comput. 5 (1984) 1–20.

[25] G. B. Whitham, Linear and Nonlinear Waves, Wiley-Interscience, New York, 1974.

[26] E. F. Toro, Riemann Solvers and Numerical Methods for Fluid Dynamics, Springer, Berlin, 1999.

[27] A. Harten, High resolution schemes for hyperbolic conservation laws, J. Comput. Phys. 49 (1983) 357–393.

[28] J. W. Banks, T. D. Aslam, W. J. Rider, On sub-linear convergence for linearly degenerate waves in capturing schemes, J. Comput. Phys. 227 (2008) 6985–7002.

[29] H. Q. Yang, A. J. Przekwas, A comparative study of advanced shock-capturing schemes applied to Burgers' equation, J. Comput. Phys. 102 (1992) 139–159.